ADAPTION OF MOBILE ROBOT PLATFORM FOR COTTON HARVESTING

M.E. C. Burce
J.M. J. Maja
Clemson University
Blackville, SC
E. M. Barnes
Cotton Inc.
Cary, NC

Abstract

Robots are becoming more integrated in the manufacturing industry. Though, most of the manufacturing environment is not as complicated as outdoor, recent advances on sensors and algorithm provide an interesting outlook on how robots will be working outdoor with humans. Commercial small unmanned ground vehicle (UGV) or mobile ground robots with navigation sensing modality provides a platform to increase farm management efficiency. The platform can be retrofitted with different manifolds that perform a specific task, e.g., spraying, scouting (having multiple sensors), phenotyping, harvesting, etc. This paper will present a robot prototype which can be used for selective harvesting of cotton. In this paper, an autonomous map-based robot navigation will be presented including an initial result for selective harvesting experiment. A graphical user interface was created which allow the user to specify way points or segments on a field. These points/segments can be represented in different scenarios, e.g. locations of mature cotton bolls, locations of weeds, insects, etc. The robot will autonomously navigate to these segments and performs the task, in this paper selective harvesting of the cotton bolls. The robot was retrofitted with a vacuum-type system with a small storage bin. Performance test on navigation and the vacuum harvesting will be presented.

Introduction

Robots are becoming more integrated in the manufacturing industry. Some examples of these integrations include material handling gantry robots (Fleisch et al., 2019), autonomous transport vehicles (Martin et al., 2019), automotive kitting applications (Krueger et al., 2019), TIREBOT (Levratti et al., 2019), and iRobot-Factory (Hu et al., 2019). Zielinska (2019) classified these industrial robots as those that operate under fully structured environments. However, field robots like those in the agriculture industry, work in fully unstructured natural environments. Though, most of the manufacturing environment is not complicated as outdoor, recent advances in sensors and algorithms provide an interesting outlook on how robots will be working outdoor with humans.

Robots are also applied in other industries (services, construction, mining, transportation/communication, agriculture/forestry/fishery) for smart factories, smart buildings, smart homes, smart cities, and even on smart farms where it employs new paradigms and technologies like Industry 4.0, internet of things (IoT), cyber-physical systems (CPS), artificial intelligence (AI) and machine learning (ML). In smart farms, several technologies like unmanned aerial systems (UAS), unmanned ground vehicles (UGV) or mobile ground robots, GPS, remote sensing, sensor fusion, and others are utilized to further improve crops agronomic performance. In the textile industry, for example, growers of cotton (*Gossypium spp.*) aim for optimized fiber yield and quality (Schielack et al., 2016). The need for the textile industry and advances in robotics has led to the proliferation and use of mobile robot platforms applied to the cotton industry. Several applications of robot platforms have been studied in cotton phenotyping (Xu et al., 2018; Jung et al., 2018; Jiang et al., 2016); lint yield prediction (Haghverdi et al., 2018), path tracking (Zhang et al., 2018; Huang et al., 2018), monitoring germination (Chen et al., 2018); wireless tracking of cotton modules (Sjolander et al., 2011), yield prediction (Maja et al., 2016); yield monitoring (Sui et al., 2004; Wallace, 1999), and cotton residue collection (Ntogkoulis et al., 2014). Cotton growers who applied various technologies reported increased field performance and efficient use of resources (Daystar et al., 2016).

As such, a strategic collaborative project between Cotton Inc. and Clemson University Edisto REC was initiated to explore the development of a mobile robot platform for cotton harvesting applications. The mobile robot platform is expected to have an autonomous map-based navigation system with a graphical user interface allowing users to specify points or segments on a mapped field. These points/segments can be represented in different scenarios, e.g. locations of mature cotton bolls, locations of weeds, insects, etc. where the mobile robot will navigate to perform some specific task, allowing a degree of control by its user. In this study, a small commercial UGV or mobile ground robot was explored as a platform for the selective harvesting of cotton bolls. Our objective includes programming the robot to navigate within plant rows, develop a harvesting mechanism mounted on the robot and evaluate its performance. Initial results of ongoing research and preliminary lab and field trials are presented.

Materials and Methods

Mobile Robot Platform

The robot used in this work is the Husky A200 from Clearpath Robotics. The robot is suitable for field operations as its width of 27 inches fits common cotton row spacings. It is lightweight for field traffic and thus soil compaction is not an issue as compared to huge farm machines. The robot is powerful enough to handle payloads of up to 165 lbs. and can operate at speeds of 3 fps. It has a 24VDC Lead-acid battery which can provide 3 hours of operation. It comes equipped with IMU (CHR-UM7, CHRobotics, Australia), GPS (Novatel Smart6-L, Novatel, Canada), individual steering motors and encoders for each wheel for basic navigation and a laser scanner (UST-10LX, Hokuyo, Japan) for obstacle detection. The robot can be programmed to perform specific tasks like mapping, navigation, and obstacle avoidance through its onboard PC running on Ubuntu 14.04 operating system and the Robot Operating System (ROS, Indigo version) framework. A mini LCD screen, keyboard and pointing device was connected to the onboard PC allowing the user to write code, view and perform operations, like selecting points on the generated map for the robot to navigate to. The harvesting system or harvester that is mounted on top of the robot is described in the next section.

Harvester System

A vacuum-type harvester was developed that uses a blower motor (McMaster 12Vdc 12A, 1000 rpm and 250 CFM) attached on top of a 5-gallon bin. The blower's 4-inch diameter inlet port was connected to the top cover of the bin through a rubber hose. On one side of the bin, a hole was made to fit a 6-feet corrugated hose with a 1.25-inch diameter opening. At the tip of the hose was a 3D-printed nozzle tied to an extrusion frame that extends on one side of the robot. The nozzle's position was fixed prior to harvesting operations to where most cotton bolls were situated along the plant row. A custom-built controller board (AtMega 644P, Microchip, USA) interfaced to the robot's onboard PC controls the blower motor and the light blinker that serves as a warning device during operation. The controller board, blower and blinker are powered by an external 12Vdc lithium polymer battery. All the harvester components were attached to an aluminum extrusion assembly frame that can be easily retrofitted to the robot's frame. The combined setup of the mounted harvester integrated on the mobile robot platform is shown in Figure 1.

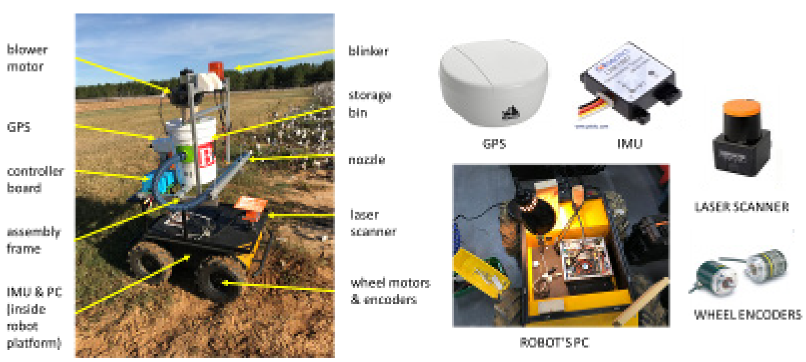

Figure 1. Mobile robot platform with harvester for cotton.

Field Navigation and Harvesting

Autonomous field navigation is achieved by having a digital map of the field and localizing the robot on that map. Localization involves integrating the coordinate frame of the robot with the coordinate frame of the digital map. The robot's coordinate frame, commonly referred as its odometry, estimates the robot's position and orientation over time. The accuracy of the robot's odometry may be enhanced by integrating it with other positional readings from an IMU or a GPS device. The robot's position is first determined using the kinematic model in Figure 2. The kinematic model of the four-wheeled robot used in this study was treated as a two-wheeled differential robot with virtual wheels W_L an W_R to simplify calculations. The robot's current position is determined by a tuple (x_c, y_c, ±) and its new position (x_c, y_c, ±)' after time ´*t,* given its right and left virtual wheel linear speeds, v_R and v_L, respectively. The linear speed of each virtual wheel is shown in Equation (1) and (2).

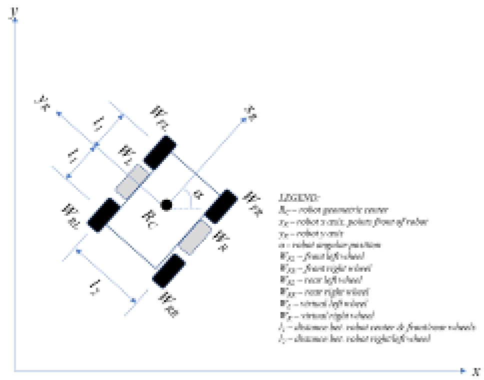

Figure 2. Kinematics of robot to determine robot's current position.

$$v_R = É_{W_R} \times r \qquad (1)$$
$$v_L = É_{W_L} \times r \qquad (2)$$

where *É* is the angular speed and *r* is the wheel radius. The angular speeds *É* and angular position *Æ*of each virtual wheel is the average of its real counterparts as shown in Equations (3) to (6),

$$Æ_{W_L} = (Æ_{W_{FL}} + Æ_{W_{RL}})/\,2 \qquad (3)$$
$$Æ_{W_R} = (Æ_{W_{FR}} + Æ_{W_{RR}})/\,2 \qquad (4)$$
$$É_{W_L} = (É_{W_{FL}} + É_{W_{RL}})/\,2 \qquad (5)$$
$$É_{W_R} = (É_{W_{FR}} + É_{W_{RR}})/\,2 \qquad (6)$$

The robot's angular speed and position are shown in Equations (7) and (8),

$$± = (Æ_{W_R} - Æ_{W_L}) \times (r\,/\,l_2) \qquad (7)$$
$$¬ = d±/\,dt \qquad (8)$$

and Equations (9) and (10) computes the robot's *x* and *y* component,

$$‹_c = (v_L + ¬(l_2/2))\ cos\ (±) \qquad (9)$$
$$_c = (v_L + ¬(l_2/2))\ sin\ (±) \qquad (10)$$

and to get the actual position we compute Equations (11) and (12),

$$x_c = +_0^t ‹_c\, dt \qquad (11)$$
$$y_c = +_0^t {}_c\, dt \qquad (12)$$

A YAML file in ROS contains the common robot configuration settings that can be loaded and referenced by other applications. Usually, the predefined values of each variable are initially inputted by the user into the robot's YAML configuration file. The YAML file is one of the many files that the user needs to setup to correctly configure the

ROS Navigation Stack on the robot's PC. The ROS Navigation Stack is an integrated framework of individual software or algorithmic packages bundled together as nodes for steering the robot from one point to the next as shown in Figure 3a. Users configure the navigation stack by either plugging-in built-in or custom-built packages in any of the nodes of the navigation stack. Estimation of the robot's odometry is therefore handled internally by the nodes in the navigation stack that automatically loads, references and updates the YAML file during runtime execution of the robot.

In this study, the digital map of the field was generated using a GMapping algorithm, a variant of simultaneous localization and mapping (SLAM) algorithm as discussed by Grisetti et al. (2005, 2007). GMapping involved fusing the robot's odometry, GPS, IMU and laser scanner readings using Kalman filters and Rao-Blackwell particle filters (RBPF) to determine the robot's current position and orientation on the map. To fuse all the sensor readings, the ROS *robot_localization* package (Charles River Analytics, Inc.) containing non-linear state estimation nodes that keeps tracks of the 15-dimensional state of the robot: $(X,Y,Z,roll,pitch,yaw,\dot{X},\dot{Y},\dot{Z},\dot{roll},\dot{pitch},\dot{yaw},\ddot{X},\ddot{Y},\ddot{Z})$. These nodes use an omni-directional motion model to project the state forward in time and corrects that projected estimate using perceived sensor data (ROS Wiki). The *ekf_se_odom* node filters all continuous data from the IMU and wheel odometry while the *ekf_se_map* node fuses all discrete data from the GPS and other data sources. Another node, the *navsat_transform* node converts the raw GPS data into odometry messages and publishes the Universal Transverse Mercator (UTM) coordinate frame to the robot's odometry frame. The data from the three nodes, which specifies the robot's currents pose (position and orientation) in the map is utilized by the *move_base* node to generate the velocity commands for the robot's movement to a target position based on its global and local path planning algorithms.

A custom-built global/local planner package was then developed suitable for steering the robot within plant rows and avoiding obstacles using the laser scanner. To navigate, a graphical user interface (GUI) showing the map of the field allows users to either click points or segments on the map or hardcode the GPS coordinates (longitude and latitude) in a text file where the robot will move. The inputted GPS coordinates or the selected points/segments on the map are then translated to the robot's coordinates specifying the desired target pose (x and y positions, and yaw orientation). These coordinates are then passed as navigation goals to the *move_base* node. The *move_base* node then determines the current robot pose and generates a path plan that will command the robot to navigate autonomously to the desired goal position. These goal positions could be the locations of the cotton bolls to be harvested. A screenshot example of the GUI interface (Figure 3b) shows the generated map of the plant rows with the robot and its navigation tracks. The navigation buttons at the top left of the GUI allow the user to click the buttons and specify the actual and starting position of the robot on the map (2D Pose Estimate) and the target goal position as to where along the plant row will the robot will go (2D Nav goal).

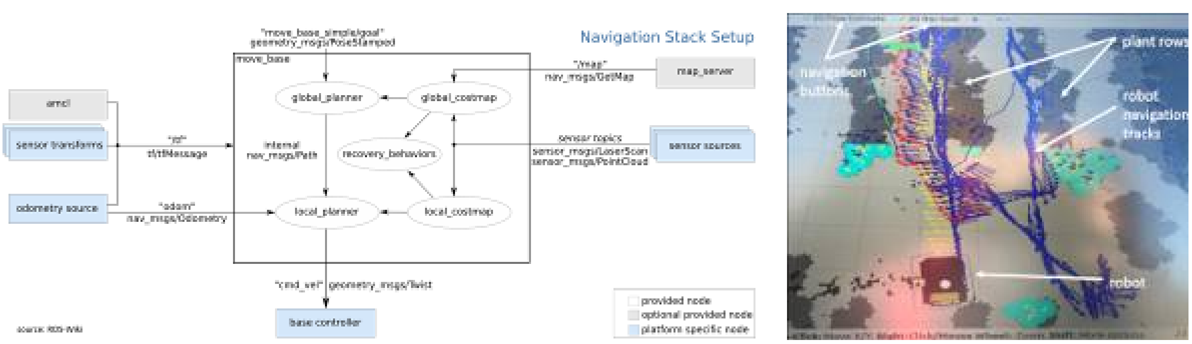

(a) (b)

Figure 3. ROS Navigation Stack in (a) and sample GUI interface showing GMapping generated map of plant rows, robot, robot tracks, and navigation buttons in (b).

To harvest the cotton bolls on the plant, a common reference coordinate was first established between the robot base with respect to the plant location as shown in Figure 4. Both the relative positions of the cotton bolls and the nozzle was then defined from this reference coordinate. Prior to harvesting, the average boll heights and boll offsets for each row or plot to be sampled was measured to calibrate the position of the nozzle. The calibration will place the nozzle in a position where most of the cotton bolls are located along the plant row. The robot was then programmed to keep track of its relative position away from the plant as it navigates along the rows. The robot also monitored the points/segments defined by the user which signals the activation or deactivation of the blower motor and blinker to start or end the harvesting.

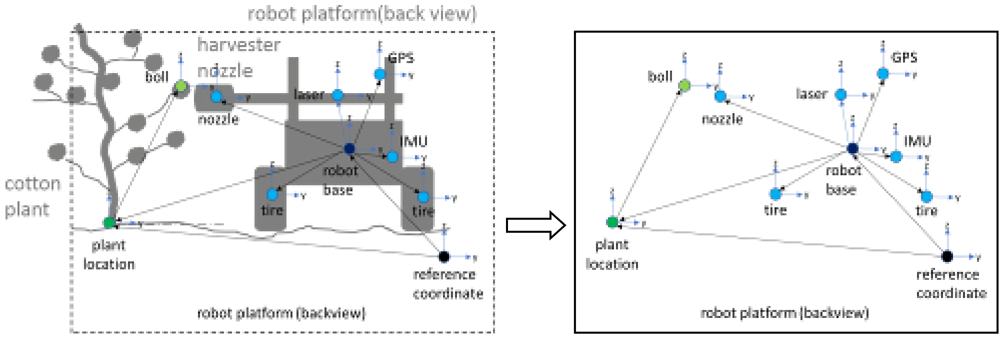

Figure 4. Relative positions of harvester nozzle versus cotton bolls concerning robot base and plant location under a common reference coordinate.

Study Site

At 270 x 465 foot, the 29-row loamy sand field of cotton (Deltapine 1358 B2XF) was established with 38 inch row spacing and 4 inch in-row plant spacing at the Edisto Research and Education Center in Blackville, SC. Seeding was done on May 16, 2018 and harvesting in the first week of December 2018. Regular crop management practices were applied during the growing season. Laboratory and field tests were conducted to configure and evaluate the performance of the navigation and harvesting system before they were integrated.

Performance Evaluation

The performance of the robot in cotton harvesting was first evaluated in the laboratory in terms of how effective the harvester suctions the cotton bolls and how close should it be to the nozzle. Results of these tests will help calibrate the positioning of the robot relative to the plant and the positioning of the nozzle during the actual field harvesting. Two rows in the field were initially identified as sampling rows. Ten cotton plant samples per row were taken to the lab. Each plant's stem was cut above ground with all other parts of the plant intact. Plant samples were taken approximately two weeks after defoliation.

Lab tests for effective suctioning distance

Ten random cotton bolls per row were selected from the plant samples. Each cotton boll has about 4 to 5 locks. The nozzle was clamped to a vise grip and a ruler placed alongside its front opening to determine the suction distance. The blower motor was activated manually before individual cotton bolls were hand-drawn closer to the nozzle until it got suctioned. The distance between the nozzle's tip and edge of the cotton boll facing the nozzle was then measured and recorded.

Lab tests for suctioning locks per boll

A lab setup that simulated an actual harvesting was conducted. Plants were lined-up and mounted in a makeshift rack inside the lab. Ten random cotton bolls per row were selected from the plant samples. Bolls of each plant targeted for harvesting were all aligned along the traversal path of the nozzle. The robot was then programmed to traverse along the simulated plant row with the harvester activated. A traversal speed of 0.5 m/s, like actual harvesting, was applied. Number of locks successfully suctioned per boll per plant were recorded at the end of each robot's pass. There were about five robot passes for each boll. On each pass, either the plant or the nozzle's position was adjusted so that all the locks on a boll will be tested for harvesting. Scoring for each boll is the ratio between the number of locks suctioned over total number of locks for that boll.

Actual field test was conducted a week after the laboratory tests. Harvesting performance of the robot was evaluated by counting the number of cotton bolls that were harvested on the sampled rows. The same two rows in the field were samples taken for the laboratory tests were also used selected.

Field tests for harvester performance
Cotton boll yield sampling based on Goodman et al. (2003) was applied during the field tests. Two 10-row feet (RA and RB) sampling locations were selected and then subdivided into three subplots. The subplots were labeled RA1 to RA3 and RB1 to RB3, as shown in Figure 5(a). Each subplot has 10 consecutive cotton plants. The 10-row feet was subdivided into subplots to account for the variabilities observed at the time of the measurements. Differences in plant height and cotton boll opening along the row were visually observed. To determine the position of the cotton bolls on each plant, measurements were made on the plant height, boll distance from stem (boll offset), and boll height above ground. These measurements were used to calibrate the position of the harvester nozzle targeting where most of the bolls are located as shown in Figure 5(b). Measurements were all done two to three weeks after defoliation.

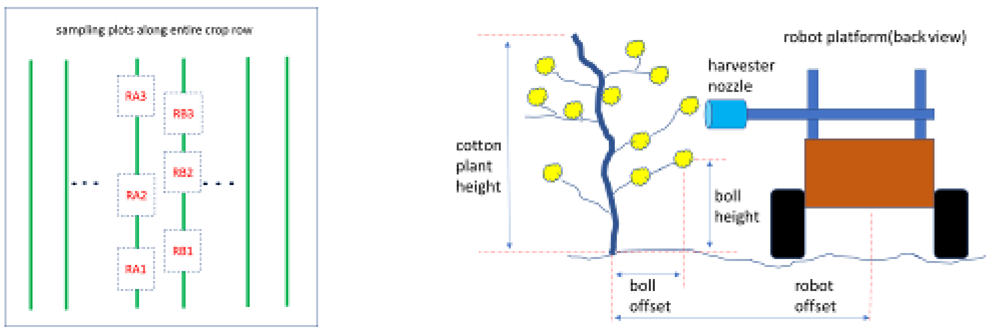

(a) (b)

Figure 5. Random sampling plot design for cotton boll harvesting in (a) and sampling measurements for boll position to determine the position of the fixed nozzle in (b).

Results and Discussion

The preliminary results of the lab and field trials for the system configuration and performance evaluation are presented in this section. These results were based on the first six months of prototype development of the ongoing project.

Performance Evaluation

Lab tests for effective suctioning distance
For the developed suction system, most of the locks were suctioned-off the boll half an inch away from the nozzle. Figure 6a shows the average offset distance of 0.48 and 0.46 inches for rows A and B, respectively. Results indicate that the developed harvester does not have enough vacuum power to suction the entire boll; however, it is strong enough to suction the locks on each boll. Normally, only one lock is suctioned-off from each boll. In some instances, two locks were suctioned when both locks were close to the nozzle.

Lab test for suctioning locks per boll
Figure 6b shows that Row B performed better with 52.5% of the locks suctioned compared to 45.5% of Row A. Averaging both performances results in 49% harvesting performance in the lab test conducted. Locks on Row A were observed to have more partially opened/immature bolls compared to those of Row B, where most bolls were fully opened/mature. The partially opened bolls grip the locks more inside the bur making it difficult for the harvester to suction.

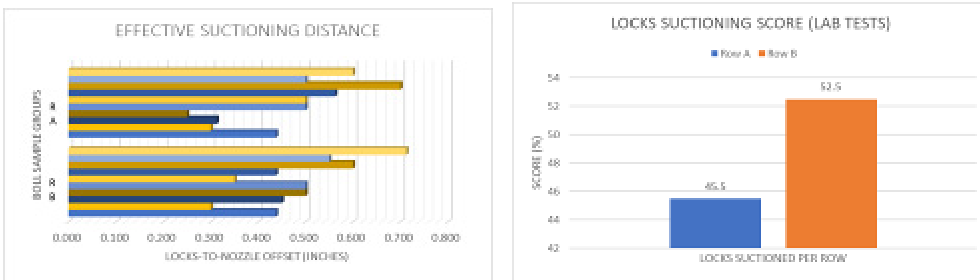

(a) (b)

Figure 6. Results of how close the locks/boll should be to the nozzle for suctioning in (a) and percentage of locks suctioned per sampled row in (b).

Field tests for harvester performance

Results show that the average plant height in all subplots was 40.92±4.70 inches as shown in Figure 7(a). Average boll offset was 10.41±4.52 inches and boll height were 23.42±4.08 inches as shown in Figure 7(b). The boll offset and boll height results indicate the region where most of the bolls are located and where the nozzle should be positioned. However, due to design constraints, the nozzle could only be adjusted vertically 18-27 inches in the vertical direction. We observed that per subplot, there were approximately 4.5 bolls on an average per plant that was in this adjustment range. So, with 30 plants per row, a total of 135 bolls were possibly harvestable.

Out of 135 bolls, we roughly estimated that approximately 20% of it is in the direct path of the nozzle's linear movement as it passes the plants. Hence, we expected 27 bolls to be harvested per row. However, based on the lab tests results conducted, the current configuration of the harvester only allows one lock per boll to be suctioned. Therefore, 27 locks are expected instead of 27 bolls. Results shows that Row A have 11 locks (40.7%), and Row B 20 locks (74.1%) harvested in total as shown in Figure 8. The average weight of each lock was 0.027 and 0.030 oz for Rows A and B, respectively. In Row B, more locks per boll were harvested since in this row; the plants have more fully opened/mature bolls compared to Row A. The results in the field tests agree with the results conducted in the lab tests where Row B performed better.

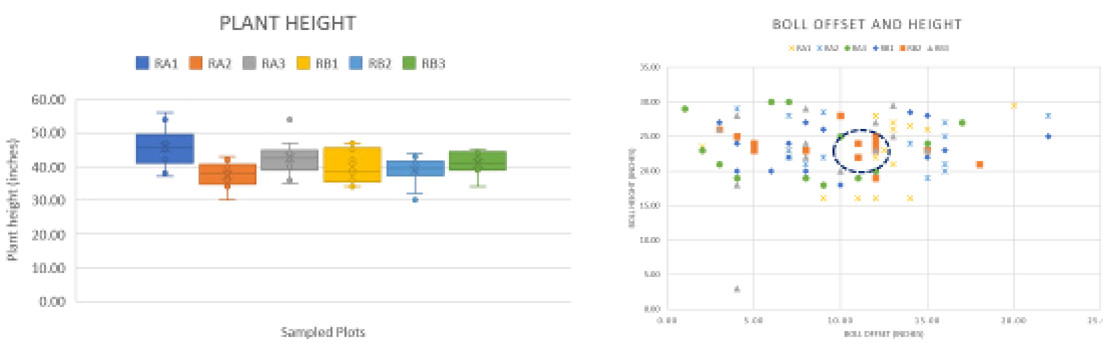

(a) (b)

Figure 7. Results of the plant height (a), boll offset and boll height (b).

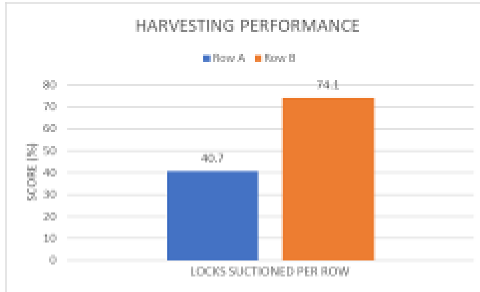

Figure 8. Field performance result of the mobile robot platform.

Summary

Preliminary results on the performance of the developed mobile robot platform for cotton harvesting shows an average of 57.4% success rate in harvesting locks that are about half an inch close to the harvester nozzle. Field test results show that the average plant height is 40.92±4.70 inches while the average boll offset is 10.41±4.52 inches and average boll height is 22.5 inches. For lab tests, results revealed that the average suction distance of the boll/locks to the harvester nozzle is 23.42±4 inches and a 49% harvesting performance in lab tests. Further improvements in the design and implementation of both the navigation and harvester system are needed to make it suitable for farm applications. More efficient navigation algorithms, more advanced sensors, and actuators are to be integrated to improve the harvesting performance of the robot platform.

Acknowledgments

The authors express their gratitude to the Cotton Inc. for funding this research under Project No. 17-029. Also, this material is based upon work supported by NIFA/USDA, under Project number SC-1700540. Mention of specific products is for information only and not for the exclusion of others that may be suitable.

References

Chen, R., T. Chu, J. Landivar. 2018. Monitoring cotton (Gossypium hirsutum L.) germination using ultrahigh-resolution UAS images. Precision Agriculture, 19, 161-177.

Daystar, J., E. Barnes, K. Hake, R. Kurtz. 2016. Sustainability Trends and Natural Resource Use. In U.S. Cotton Production. Bioresources, North America, 12, Nov. 2016. Available at: <Http://Ojs.Cnr.Ncsu.Edu/Index.Php/Biores/Article/View/Biores_12_1_362_Daystar_Sustainability_Trends_Cotton_Production>. Date Accessed: 01 Jan. 2019.

Fleisch, R., D. Entner, T. Prante, R. Pfefferkorn. 2019. In Andres-Perez, E., et al. (eds.). Evolutionary and Deterministic Methods for Design Optimization and Control with Applications to Industrial and Societal Problems, Computation Methods in Applied Sciences, 49, 339-354.

Goodman, B., and C.D. Monks. 2003. A farm demonstrations method for estimating cotton yield in the field for use by extension agents and specialists. Journal of Extension, Vol. 41, No. 6.

Grisetti, G., C. Stachniss, W. Burgard. 2007. Improved Techniques for Grid Mapping with Rao-Blackwellized Particle Filters, IEEE Transactions on Robotics, Volume 23, pages 34-46.

Grisetti G., C. Stachniss, W. Burgard. 2005. Improving Grid-based SLAM with Rao-Blackwellized Particle Filters by Adaptive Proposals and Selective Resampling, In Proc. of the IEEE International Conference on Robotics and Automation (ICRA.

Haghverdi, A., R. Washington-Allen, B. Leib. 2018. Prediction of cotton lint yield from phenology of crop indices using artificial neural networks. Computers and Electronics in Agriculture, 152, 186-197.

Hu, L., Y. Miao, G. Wu, M. Hassan, I. Humar. 2019. iRobot-Factory: An intelligent robot factory based on cognitive manufacturing and edge computing. Future Generation Computer Systems, 90, 569-577.

Huang, P., Z. Zhang, X. Luo, J. Zhang, P. Huang. 2018. Path tracking control of a differential-drive tracked robot based on look-ahead distance. IFAC PapersOnline, 51-17, 112-117.

Jiang, Y., C. Li, J. S. Robertson, S. Sun, R. Xu, A.H. Paterson. 2018. GPhenoVision: A ground mobile system with multi-modal imaging for field-based high throughput phenotyping of cotton. Scientific Reports, 8, Art. No. 1213.

Jiang, Y., C. Li, A. H. Paterson. 2016. High throughput phenotyping of cotton plant height using depth images under field conditions. Computers and Electronics in Agriculture, 130, 57–68.

Jung, J., M. Maeda, A. Chang, J. Landivar, J. Yeom, J. McGinty. 2018. Unmanned aerial system assisted framework for the selection of high yielding cotton genotypes. Computers and Electronics in Agriculture, 152, 74–81.

Krueger, V., F. Rovida, B. Grossman, R. Petrick, M. Crosby, A. Charzoule, G.M. Garcia, S. Bhenke, C. Toscano, G. Veiga. 2019. Robotics and Computer Integrated Manufacturing, 57, 213-229.

Levratti, A., G. Riggio, C. Fantuzzi, A.D. Vuono, C. Sechhi. 2019. TIREBOT: A collaborative robot for the tire workshop. Robotics and Computer Integrated Manufacturing, 57, 129-137.

Maja, J., T. Campbell, J.C. Neto, P. Astillo. 2016. Predicting cotton yield of small field plots in a cotton breeding program using UAV imagery data. Proceedings Volume 9866, Autonomous Air and Ground Sensing Systems for Agricultural Optimization and Phenotyping; 98660C (2016) https://doi.org/10.1117/12.2228929

Martin, J., O. Casquero, B. Fortes, M. Marcos. 2018. A generic multi-layer architecture based on ROS-JADE integration for autonomous transport vehicles. Sensors, 19, 69, 1-16.

Ntogkoulis, P.A., D.D. Bochtis, S. Fountas, R. Berruto, T.A. Gemtos. 2014. Performance of cotton residue collection machinery. Biosystems Engineering, 119, 25-34.

Schielack, V.P., J.A. Thomasson, R. Sui, Y. Ge. 2016. Harvester-based sensing system for cotton fiber-quality mapping. Journal of Cotton Science. 20:386-393.

Sjolander, A.J., J.A. Thomasson, R. Sui, Y. Ge. 2011. Wireless tracking of cotton modules. Part 2: Automatic machine identification and system testing. Computers and Electronics in Agriculture, 75, 34–43.

Sui, R., J.A. Thomasson, R. Mehrle, M. Dale, C. Perry, G. Rains. Mississippi cotton yield monitor: beta test for commercialization. Computers and Electronics in Agriculture, 42, 149–160.

Wallace, T.P. 1999. Small plot evaluation of an electro-optical cotton yield monitor. Computers and Electronics in Agriculture, 23, 1–8.

Xu, R., C. Li, J.M. Velni. 2018. Development of an autonomous ground robot for field high throughput phenotyping. IFAC PapersOnline, 51-17, 70-74.

Zang, S., Y. Wang, Z. Zhu, Z. Li, Y. Du, E. Mao. 2018. Tractor path tracking control based on binocular vision. Information Processing in Agriculture, 5, 422–432.

Zielinska, T. 2019. History of service robots and new trends. In Novel Design and Applications of Robotics Technologies. IGI Global. 158-187.